IEEE Access
Multidisciplinary | Rapid Review | Open Access Journal

Received February 2, 2021, accepted February 10, 2021, date of publication February 16, 2021, date of current version March 1, 2021.

Digital Object Identifier 10.1109/ACCESS.2021.3059935

Fault Location of VSC Based DC Distribution Network Based on Traveling Wave Differential Current With Hausdorff Distance and Cubic Spline Interpolation

YANFANG WEI[1], PENGYU SUN[1], ZHUOLIANG SONG[2], PENG WANG[3], (Member, IEEE), ZHIHUI ZENG[1], AND XIAOWEI WANG[1], (Member, IEEE)

[1]School of Electrical Engineering and Automation, Henan Polytechnic University, Jiaozuo 454000, China
[2]Department of Electrical and Computer Engineering, University of Southern California, Los Angeles, CA 90007, USA
[3]State Grid Henan Electric Power Research Institute, Zhengzhou 450052, China

Corresponding author: Pengyu Sun (spy296212805@163.com)

This work was supported in part by the National Natural Science Foundation of China under Grant 61703144, Grant U1804143, and Grant 61403127; in part by the project of Innovative Team of Mine Power Electronic Device and Control in Henan Province under Grant CXTD2017085, and in part by the Key Scientific and Technological Project in Henan Province under Grant 182102210051.

ABSTRACT Compared with AC power system, DC distribution network is a low-damping system without natural zero crossing. The DC fault current will reach its peak value within a few milliseconds, posing a great threat to power electronic devices. Therefore, the rapid and high-precision identification of DC line faults is one of the technical difficulties faced by the VSC based DC distribution network. In this paper, a new fault location method based on traveling wave differential current with Hausdorff distance and cubic spline interpolation is proposed. First, the forward and reverse traveling waves at both ends of the VSC based DC lines are extracted, the Karenbauer transform is used to decouple the positive and negative electrodes to obtain accurate fault information. Then, the internal relationship between the differential current and the fault current is obtained according to the principle of traveling wave transmission invariance, the cubic spline interpolation algorithm is used to solve the traditional sampling frequency limitation, and the positive differential current in the interception time window is smoothly displaced. At last, the Hausdorff distance algorithm is used to analyze the correlation between the translational differential current and the reverse differential current. The fault location corresponds to the highest correlation. The proposed method uses the time-domain information at both ends of the VSC based DC lines, and it is less affected by the transition resistance. Lots of simulation experiments prove that it has a strong anti-noise interference ability and high reliability, and is less affected by the sampling frequency after cubic spline interpolation. Compared with traveling wave algorithm based on Pearson correlation coefficient, the method in this paper shows a significantly shortened error, 27% on average.

INDEX TERMS VSC based DC distribution network, fault location, traveling wave differential current, Hausdorff distance, cubic spline interpolation.

I. INTRODUCTION

With the rapid development and construction of cities, the continuous increase of urban loads puts forward higher requirements on the power supply reliability and power quality of the traditional AC distribution network, and brings a series of problems to the traditional AC distribution network [1], [2]. Compared with the AC network, the voltage source converter (VSC) based DC distribution network has the advantages of large power supply capacity, high power quality, low line loss, high power supply reliability, low investment cost, flexible control, and suitable for efficient grid connection of distributed power sources [3], [4]. So it has received widespread attention all over the world, and has

The associate editor coordinating the review of this manuscript and approving it for publication was Zhigang Liu.

This work is licensed under a Creative Commons Attribution 4.0 License. For more information, see https://creativecommons.org/licenses/by/4.0/

become a hot spot for scholars in recent years. However, the development of VSC based DC distribution system still faces several key technical problems, among which fault detection and location method is one of the key technical problems that limit its development [5], [6]. Therefore, for the VSC based DC distribution network, quickly and accurately determining the fault location is of great significance to ensure the safe and reliable operation of the power system [7].

At present, fault location technology of AC power system and HVDC transmission system is relatively mature. The VSC based DC system is a low-damping and low-inertia system, and its impedance of transmission line is very small. The faults of the system will lead to a rapid rise of current and a sudden drop of voltage [7]. Therefore, the transmission line fault should be removed as soon as possible. For the VSC based DC distribution system, due to the difference between its topology and fault characteristics and the AC system, various fault location methods based on sequence components in the traditional AC power system are no longer applicable. Traditional protection methods employed in AC systems, such as impedance relays, are not applicable for VSC based DC protection [8]. In [8], the fast dyadic wavelet transform was proposed; however, the method need to deal with a large amount of data, and the computing speed may be affected. In [9], voltage derivative scheme was used for DC fault detection, but the method was very sensitive to noise interference. Overcurrent protection for VSC-HVDC system had been studied in [10]. However, the method requires a high-current threshold value and has low accuracy of high resistance fault identification.

Traveling wave based line fault-location strategy has been successfully applied to transmission line fault location in the conventional HVDC systems. The traveling wave method is adopted for VSC-HVDC in actual power grid by ABB and SIEMENS [11]. In [7], the differential voltage traveling wave using convolution was given, and a data out-of-sync detection methodology only using the electrical quantities on both ends of the VSC-HVDC transmission line was discussed. In [12], a principle of non-unit travelling wave for DC transmission line based on waveform correlation calculation was proposed. In [13], a traveling wave detection method based on the symmetrical components was proposed. However, there are several disadvantages for traveling wave method, such as no fault direction identification capability, threshold issue and grounding resistance. Therefore, in [14], a new travelling wave directional pilot protection was proposed, which had the abilities to discriminate fault direction and discriminate fault section reliably. These algorithms take into account the response speed and selectivity of VSC-HVDC protection.

Moreover, because the DC distribution network has a low voltage level and is susceptible to noise interference, the parameter identification-based fault location methods commonly used in HVDC transmission systems also have certain limitations [15], [16]. In [17], the relationship between the natural frequency of the traveling wave and the reflection between the fault point and the beginning of the line was analyzed, and a single-ended fault location scheme was proposed. In [18], the fault location accuracy by introducing artificial neural networks was improved. In [19], the machine learning was applied to fault location, but these methods require a large amount of learning sample data. In [20], a fault location algorithm based on current measurement unit was proposed, which used state evaluation and elimination technology to eliminate non-faulty sections. After determining the most probable fault line, the fault location was calculated separately to obtain accurate results. It obtained a high location accuracy, but the amount of calculation required was relatively large. In [21], the transient travelling wave was used to locate the fault in the transmission time between the measurement point and the fault point. In [22], the similarity of the traveling wave difference current for HVDC was proposed to obtain accurate fault location information based on the traveling wave method. The traveling wave method has high location accuracy. However, the methods of [20]–[22] require high sampling frequency, and the location errors are large at low sampling frequency. This problem was solved in [23], the frequency domain method of DC transmission line fault location principle was proposed, which reduced the requirements for sampling accuracy. However, the method is only suitable for HVDC transmission lines. For VSC based DC distribution network, the transmission line is short and the measurement error is large, so the method cannot be applied well.

The waveform similarity comparison algorithm based on Hausdorff distance has the advantages of short time window and small amount of calculation, and has been widely used in geometric modeling, image recognition and other fields [24], [25]. It has been introduced into the field of power system by experts and scholars. It is mainly used to measure the similarity between graphs, i.e. image matching. The algorithm considers the difference of overall characteristics of waveforms and discards the detailed features of graphs. To protect the DC line of VSC based DC system, this paper proposed a novel VSC based DC distribution system fault location algorithm based on traveling wave differential current with Hausdorff distance and cubic spline interpolation. The main contribution of this paper are summarized as follows:

(1) The new method is based on the characteristics of traveling wave differential current and can accurately reflect the fault location. The analysis of waveform similarity between positive and negative differential currents and fault point current are included. The Karenbauer transform is used to decouple the positive and negative poles to obtain accurate fault information, and smoothly shift the forward difference current in the interception time window.

(2) The Hausdorff distance is selected to process the fault location data and it measures the matching degree between two sets of points, which has lower ranging error. By using Hausdorff distance, the similarity degree of two groups of data in the translation process can be accurately

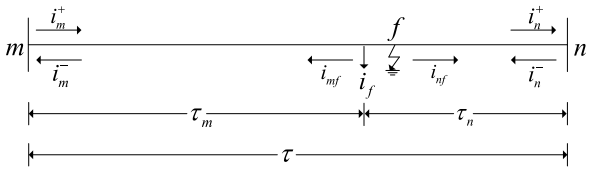

FIGURE 1. Schematic diagram of uniform traveling line fault traveling wave.

identified, and the effective information of fault location can be extracted.

(3) The cubic spline interpolation technology is used to solve the problem of large errors in traveling wave fault location at lower sampling frequencies, and to meet the requirements of the distribution network for fault location errors.

The rest of this paper is organized as follows. Fault location mechanism of traveling wave is introduced in Section 2. The new fault location algorithm based on traveling wave differential current with Hausdorff distance and cubic spline interpolation is derived in Section 3. In Section 4, the test results are given to verified the effectiveness of our fault detection method. In Section 5, we get the conclusions.

II. FAULT LOCATION MECHANISM OF TRAVELING WAVE

A schematic diagram of a faulty traveling wave in a uniform transmission line is shown in Fig. 1. The wave flows from end-m to end-n is defined as forward traveling wave. The wave flows from end-n to end-m is defined as reverse traveling wave.

The current traveling wave at both ends of mn is

$$\begin{cases} i_m^+(t) = \dfrac{u_m(t)}{Z_C} + i_m(t) \\ i_m^-(t) = \dfrac{u_m(t)}{Z_C} - i_m(t) \end{cases} \quad \begin{cases} i_n^+(t) = \dfrac{u_n(t)}{Z_C} - i_n(t) \\ i_n^-(t) = \dfrac{u_n(t)}{Z_C} + i_n(t) \end{cases} \tag{1}$$

where $i_m^+(t)$ and $i_m^-(t)$ are the forward and reverse current of traveling waves at the end-m, respectively. $i_n^+(t)$ and $i_n^-(t)$ are the forward and reverse current of traveling waves at the end-n, respectively. $u_m(t)$ and $i_m(t)$ are the voltage and current at the end-m, respectively. $u_n(t)$ and $i_n(t)$ are the voltage and current at the end-n, respectively. $i_{mf}(t)$ and $i_{nf}(t)$ are the fault current from the fault point f to point m and point n, respectively.

According to the traveling wave theory, the positive direction of the current at both ends of the line is from the bus to the line, and the current at any point in the line can be regarded as the superposition of the forward and reverse current traveling waves.

When the fault is occurred at the internal point f of the transmission line, the line is divided into line-mf and line-fn. τ_m and τ_n are the propagation delays of the traveling wave from point f to end-m and end-n, respectively.

$\Delta\tau$ is the time difference of traveling wave propagation on both sides of the fault point, and $\Delta\tau$ is

$$\begin{cases} \Delta\tau = \tau_m - \tau_n \\ \Delta\tau \in (-\tau, \tau) \end{cases} \tag{2}$$

The calculating formula of the distance from end-m to fault point f is

$$l_{mf} = \frac{\tau + \Delta\tau}{2} v \tag{3}$$

The propagation delay of the traveling wave from end-m to end-n is τ. When the line is operating in normal condition, there is

$$\begin{cases} i_m^+(t) = i_n^+(t+\tau) \\ i_m^-(t) = i_n^-(t-\tau) \end{cases} \tag{4}$$

The differential currents of forward and reverse direction of the line are

$$\begin{cases} \mathrm{d}i^+(t) = i_m^+(t-\tau) - i_n^+(t) \\ \mathrm{d}i^-(t) = i_n^-(t-\tau) - i_m^-(t) \end{cases} \tag{5}$$

After the fault occurs, the integrity of the line is destroyed, and the line-mf and the line-fn meet the transmission invariance of traveling wave respectively, the relationship between differential current and fault current is

$$\begin{cases} \mathrm{d}i^+(t) = i_f(t-\tau_m) \\ \mathrm{d}i^-(t) = i_f(t-\tau_n) \end{cases} \tag{6}$$

We shift $\mathrm{d}i^+(t)$ backward along the time axis by $\Delta\tau$ time and get the $\mathrm{d}i^+(t-\Delta\tau)$ as

$$\mathrm{d}i^+(t-\Delta\tau) = \mathrm{d}i^-(t) \tag{7}$$

In the translation process, when $\Delta t = \Delta\tau$, the waveforms of $\mathrm{d}i^+(t-\Delta\tau)$ and $\mathrm{d}i^-(t)$ have the highest similarity. Record the time Δt at this moment and substitute it in Eq.(3), then we can obtain the desired fault location result.

III. FAULT LOCATION METHOD

A. PHASE-MODE TRANSFORMATION

VSC based DC distribution lines usually consist of positive line and negative line, that is the bipolar lines. Due to the electrical coupling between the bipolar lines, it is necessary to use an appropriate matrix transformation to decouple it when analyzing the traveling wave transmission process. The Karenbauer transformation matrix can be used to decouple the voltage and current between the two poles. The results of voltage and current of the earth and aerial mode components obtained after decoupling will be no electrical coupling [26].

For n-phase transmission lines, the Karenbauer transformation matrix is

$$S = \begin{bmatrix} 1 & 1 & \cdots & 1 \\ 1 & 1-n & \cdots & 1 \\ \vdots & \vdots & & \vdots \\ 1 & 1 & \cdots & 1-n \end{bmatrix} \tag{8}$$

Take voltage traveling wave as an example. The phase-mode transformation is obtained by inverse matrix form of Karenbauer transformation matrix S. And its transformation form is

$$U_m = S^{-1}U \tag{9}$$

where U_{m} is the mode voltage vector. U is the voltage vector. S^{-1} is the inverse matrix of Karenbauer transformation.

Therefore, the Karenbauer transformation form of the DC distribution line is

$$\begin{bmatrix} u_{\mathrm{m0}} \\ u_{\mathrm{m1}} \end{bmatrix} = \frac{1}{\sqrt{2}} \begin{bmatrix} 1 & 1 \\ 1 & -1 \end{bmatrix} \begin{bmatrix} u_a \\ u_b \end{bmatrix} \tag{10}$$

where u_{m0} and u_{m1} are the earth mode and aerial mode voltage vectors, respectively. u_a and u_b are the positive and negative voltage vectors, respectively.

The parameters of DC lines have frequency-dependent characteristics. It can be seen from Eq.(3) that the accuracy of fault location is directly related to the wave speed of a certain frequency. The earth mode parameters are affected by the ground loop impedance, and its wave speed varies significantly with various frequency. For this reason, this paper uses single aerial mode component to implement the fault location algorithm.

B. HAUSDORFF DISTANCE THEORY

Hausdorff distance is a measure of similarity between two sets of points [24], [25]. For the given two sets of finite points:

$$A = \{a_1, \ldots, a_n\} \quad B = \{b_1, \ldots, b_n\} \tag{11}$$

We choose a point a_i in point set A, then we calculate the Euclidean distances between a_i and each point b_k in point set B [24]. Then we arrange them in accordance with size order and find the closest point b_j to a_i, making b_j satisfy:

$$\left\| a_i - b_j \right\| \leq \left\| a_i - b_k \right\|, \quad 1 \leq k \leq n \tag{12}$$

where $\|a - b\|$ is the Euclidean distance between a and b. b_k is a point in point set B. And $\left\|a_i - b_j\right\|$ in Eq.(12) is the minimum distance corresponding to a_i points:

$$\min_{b_k \in B} \left\| a_i - b_k \right\| = \left\| a_i - b_j \right\| \tag{13}$$

We define $h(A, B)$ as the Hausdorff unidirectional distance from A to B. For all elements in A, the maximum value satisfying Eq.(13) is:

$$h(A, B) = \max_{a_i \in A} \min_{b_j \in B} \left\| a_i - b_j \right\| \tag{14}$$

By analogy, We define $h(B, A)$ as the Hausdorff unidirectional distance from B to A. For all elements in B, the maximum value satisfying Eq.(13) is:

$$h(B, A) = \max_{b_j \in B} \min_{a_i \in A} \left\| b_j - a_i \right\| \tag{15}$$

We define $H(A, B)$ as the Hausdorff distance between A and B. It is the larger value of the Hausdorff one-way distance between A to B and B to A.

$$H(A, B) = \max(h(A, B), h(B, A)) \tag{16}$$

In the comparison of waveform similarity, the Hausdorff distance between the two sets of waveforms indicates the maximum data difference. The smaller the Hausdorff distance, the smaller the maximum data difference and the higher degree of similarity.

C. CUBIC SPLINE INTERPOLATION

The cubic spline interpolation is a function composed of several cubic polynomials in its definition domain. It has the second-order continuous derivative at the connection point. The cubic spline interpolation function has fewer interpolation times, faster interpolation speed, and easy to solve undetermined coefficients. And its interpolation curve has good smoothness and reliable stability, so it has been widely used in multi-point interpolation [27], [28].

We suppose that $n+1$ nodes are taken from interval $[a, b]$, $a = x_0 < x_1 < \cdots < x_n = b$. And the function $f(x_i) = f_i (i = 0, 1, 2, \ldots, n)$ of these nodes is given. If $S(x)$ meets the following conditions:

1) It has the second order continuous derivative in interval $[a, b]$.

2) In each subinterval of $[x_i, x_{i+1}]\,(0 \leq i \leq n-1)$, $S(x)$ is a cubic polynomial.

3) If the interpolation condition $S(x_i) = f_i, i = 0, 1, 2, \ldots, n$ is satisfied, then $S(x)$ is called cubic spline interpolation function.

The cubic spline interpolation function is a piecewise cubic polynomial, and in each subinterval $[x_i, x_{i+1}]$, there are:

$$S(x) = a_i x^3 + b_i x^2 + c_i x + d_i, \quad i = 0, 1, 2, \ldots, n-1 \tag{17}$$

where a_i, b_i, c_i, d_i are the undetermined coefficients. Therefore, from the definition of the cubic spline interpolation function, it can be seen that the solution of $S(x)$ can be get by solving the four undetermined coefficients in each minimal interval $[x_i, x_{i+1}]$. The number of minimal interval is n. So there are $4n$ unknowns need to be determined, and there must be $4n$ corresponding conditions.

Since $S(x)$ has second-order continuous derivative in interval $[a, b]$, the following continuous conditions should be met at node $x_i (i = 1, 2, \ldots, n-1)$:

$$\begin{cases} S(x_i - 0) = S(x_i + 0) \\ S'(x_i - 0) = S'(x_i + 0) \\ S''(x_i - 0) = S''(x_i + 0) \end{cases} \tag{18}$$

The $3(n-1)$ interpolation conditions can be determined by Eq.(18). $n+1$ interpolation conditions can be determined according to interpolation condition $S(x_i) = f_i, i = 0, 1, 2, \ldots, n$. So far, there are $4n-2$ conditions, and the interpolation function $S(x)$ can be solved with other two boundary conditions.

There are three common boundary conditions:

The first type of boundary condition: Given the first derivative value at two endpoints: $S'(x_0) = f'(x_0), S'(x_n) = f'(x_n)$.

The second type of boundary condition: Given the second derivative value at two endpoints: $S''(x_0) = f''(x_0), S''(x_n) = f''(x_n)$. Under special circumstances, there is $f''(x_0) = f''(x_n) = 0$, and this is called the natural boundary.

The third type of boundary condition: If $S(x)$ is a function of period b-a, then $S(x)$ satisfies the following conditions at

the endpoints:

$$\begin{cases} S(x_0+0)=S(x_n-0) \\ S'(x_0+0)=S'(x_n-0) \\ S''(x_0+0)=S''(x_n-0) \end{cases} \tag{19}$$

The spline function $S(x)$ solved in Eq.(19) is called the periodic spline function.

D. FAULT LOCATION MECHANISM OF THE NEW METHOD

According to the above analysis, the fault location mechanism of the new algorithm in this paper can be obtained:

1) The reverse traveling wave differential current $\mathrm{d}i^-(t)$ is taken as the reference standard.

2) The forward traveling wave differential current $\mathrm{d}i^+(t)$ is shifted along the time axis by Δt to get $\mathrm{d}i^+(t-\Delta t)$.

3) Compare the waveform of $\mathrm{d}i^+(t-\Delta t)$ with $\mathrm{d}i^-(t)$, and get the similarity between them.

4) When $\Delta t=\Delta\tau$, $\mathrm{d}i^+(t-\Delta t)$ and $\mathrm{d}i^-(t)$ should have the highest similarity.

5) Substitution the data obtained in $l_{mf}=\frac{\tau+\Delta\tau}{2}v$ and the fault distance is got.

The detailed implementation steps of the new algorithm is as follows:

Step 1: Obtain the voltage and current signals at both ends of the DC lines through the signal acquisition device.

Step 2: Determine whether the sampling frequency exceeds 100kHz. If yes, go to Step 3; if no, go to Step 4.

Step 3: Perform cubic spline interpolation on fault location data.

Step 4: Decouple of bipolar voltage and current using Karenbauer transformation.

Step 5: Calculate the forward and reverse traveling wave currents of two-terminal lines, and define forward and reverse differential current according to traveling wave characteristics.

Step 6: Shift the forward differential current gradually while taking the reverse difference current as a reference.

Step 7: Calculate the similarity between the forward differential current and the reverse differential current after translation via Hausdorff distance.

Step 8: Record all translation data and take the maximum value, get the corresponding translation time of the maximum value, which is the best displacement time difference.

Step 9: Substitute the best displacement time difference into the fault location formula to get the accurate fault distance.

The procedure of the new algorithm in this paper is summarized in Fig. 2.

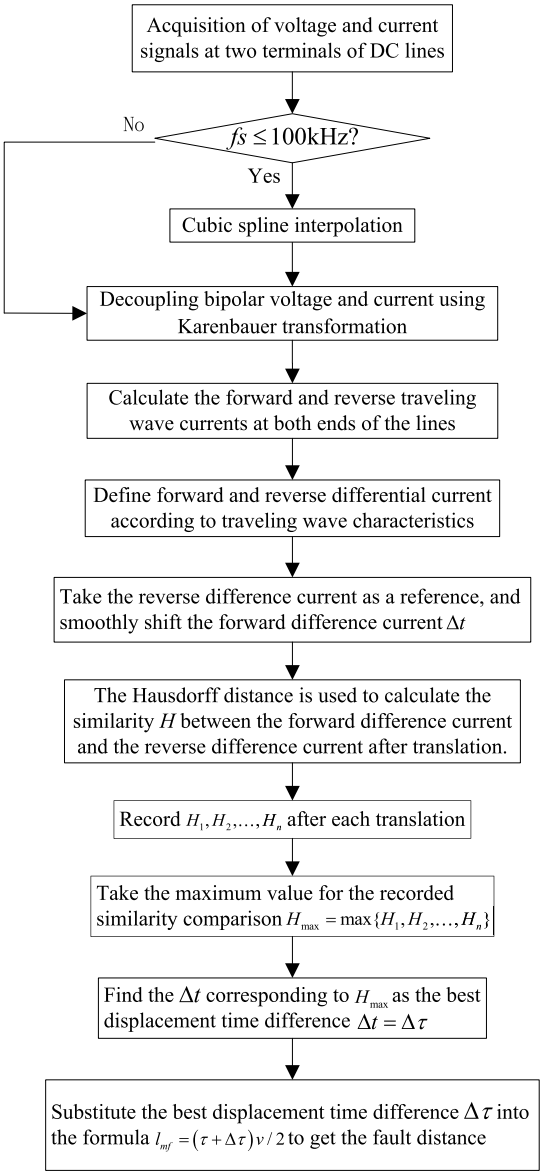

FIGURE 2. Detailed implementation steps of the new fault location algorithm.

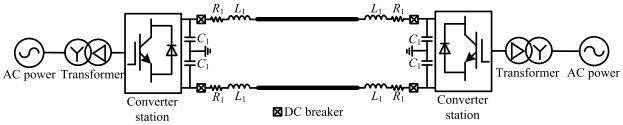

FIGURE 3. VSC based DC distribution system model.

IV. SIMULATION VERIFICATION

The VSC based DC distribution system model is shown in Fig. 3 [29]. AC power supplies and transformers are installed at the extremity of the system, which are connected to the DC lines through converter stations. DC breakers are installed at the beginning of the DC lines. In Fig. 3, C_1 represents parallel connected capacitor. L_1 and R_1 represent compensation inductor and resistance of DC lines, respectively.

A. FAULT SIMULATION ANALYSIS

As shown in Fig. 3, a ±10kV VSC based DC distribution system is built in MATLAB/Simulink, and the parameters of the system are shown in Table 1. The length of each line is

TABLE 1. Parameters of VSC based DC distribution system.

Parameters	Symbol	Value
Rated DC voltage/kV	U	10
Rated capacity/MVA	S	50
DC capacitance/F	C_1	0.01
DC resistance/Ω	R_1	0.15
DC inductance/mH	L_1	7.92
Line length/km	l	10

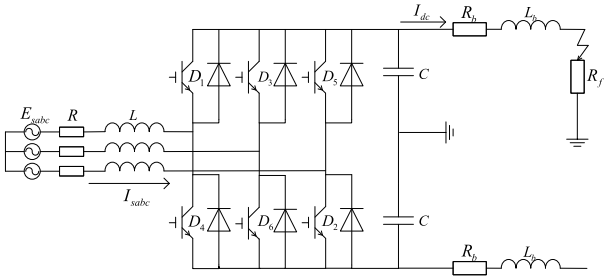

FIGURE 4. Equivalent circuit diagram with monopole grounding fault.

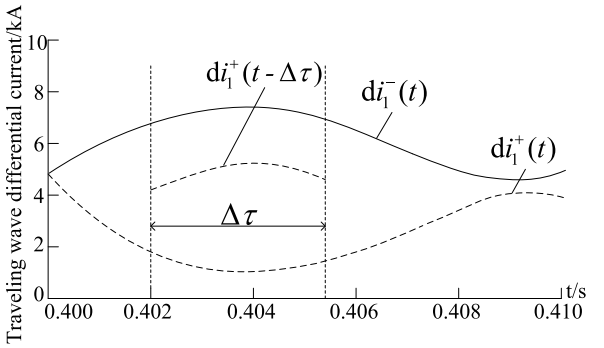

FIGURE 5. Results of fault traveling wave differential current.

10km, and the sampling frequency of the system is 200 kHz. The required data window length is 10ms. Fig. 4 is the system equivalent circuit when the system has a monopole grounding short-circuit fault. The circuit uses a three-phase full-wave bridge converter. The valve numbers of the upper half bridge are D_1, D_3, D_5, respectively, and the lower half bridge are D_2, D_4, D_6, respectively. E_{sabc} is three-phase AC power supply. I_{sabc} and I_{dc} are three-phase AC current and current of DC lines, respectively. R and L are resistance and inductance of AC system, respectively. R_b and L_b are resistance and inductance of DC lines, respectively. C is DC filter. R_f is ground resistance.

Fig. 5 is the fault traveling wave differential current after a monopole grounding short-circuit fault occurs in the VSC based DC system at 0.4s. It gives a forward differential current of aerial mode $di_1^+(t)$, a reverse differential current of aerial mode $di_1^-(t)$, and an intercepting segment of forward differential current of aerial mode after translation $di_1^+(t-\Delta\tau)$. From Fig. 5, it can be seen that there is a high similarity between $di_1^+(t-\Delta\tau)$ and $di_1^-(t)$ after translation, and the fault distance can be calculated.

TABLE 2. Fault location error under different fault distances and transition resistances.

Fault distance /km	Transition resistance /Ω	Location results /km	K_{error}/%
1	0.1	0.9832	0.168
	1	0.9686	0.314
	10	0.9462	0.538
5	0.1	4.9727	0.273
	1	4.9634	0.366
	10	4.9481	0.519
9	0.1	8.9753	0.247
	1	8.9669	0.331
	10	8.9444	0.556

B. THE INFLUENCE OF FAULT DISTANCE AND TRANSITION RESISTANCE ON THE ACCURACY OF THE NEW ALGORITHM

Three cases are considered. The distances between the bus and the fault location are set to 1km, 5km, and 9km, respectively, that is, the fault points are set at the beginning, midpoint and extremity of the transmission line. The transmission lines of the VSC based DC distribution system are usually cables, in order to analyze the influence of transition resistance on fault, so the transition resistance of the DC system is generally small. Then the transition resistances are set to be 0.1Ω, 1Ω, and 10Ω, respectively. The simulation results are shown in Table 2. The criterion for the new fault location method is given:

$$K_{\text{error}} = \frac{|\text{Measuring results} - \text{Fault distance}|}{\text{Line length}} \times 100\% < 1\% \tag{20}$$

where K_{error} is the criterion of the fault detection. 1% is the threshold value.

If the value of K_{error} exceeds the threshold value, it indicates that the failure of the method. Otherwise, the new method is successful in this case.

It can be seen from Table 2 that the fault location errors are kept within 0.556%, and the error increases with the increase of transition resistance. This is caused by the short transmission line of distribution network, and the line resistance is smaller than the transition resistance. Under various fault positions, the fault location errors are kept in a small range, indicating that the method can be applied to the whole line.

Seen from Table 2, the new fault location method proposed in this paper can obtain reliable fault location results under different fault locations and transition resistances, which can realize accurate fault location across the entire distribution network, and the positioning accuracy is less affected by the transition resistance.

TABLE 3. Fault location error under different noise interference.

SNR/dB	Fault distance /km	Transition resistance /Ω	Location results /km	K_{error}/%
0	1	0.1	0.9832	0.168
		1	0.9686	0.314
		10	0.9462	0.538
	5	0.1	4.9727	0.273
		1	4.9634	0.366
		10	4.9481	0.519
	9	0.1	8.9753	0.247
		1	8.9669	0.331
		10	8.9444	0.556
30	1	0.1	0.9774	0.226
		1	1.0357	0.357
		10	0.9458	0.542
	5	0.1	4.9666	0.334
		1	4.9634	0.426
		10	4.9481	0.594
	9	0.1	8.9753	0.461
		1	8.9669	0.507
		10	8.9444	0.686
40	1	0.1	0.9742	0.258
		1	0.9618	0.382
		10	0.9441	0.559
	5	0.1	4.9727	0.403
		1	4.9418	0.582
		10	4.9321	0.679
	9	0.1	8.9473	0.527
		1	8.9376	0.624
		10	8.9241	0.759
50	1	0.1	1.0273	0.273
		1	0.9625	0.375
		10	0.9426	0.574
	5	0.1	4.9517	0.483
		1	4.9363	0.637
		10	4.9264	0.736
	9	0.1	8.9394	0.606
		1	8.9276	0.724
		10	8.9167	0.833

C. THE INFLUENCE OF NOISE INTERFERENCE ON THE ACCURACY OF THE NEW ALGORITHM

In order to test the influence of noise interference on the accuracy of the proposed new fault location algorithm, Gaussian white noise is superimposed on the original waveform data. The signal-to-noise ratio (SNR) of the measuring device is usually not less than 30dB [30]. Table 3 shows the fault location errors under the condition of superposition of Gaussian white noise with SNR of 30, 40 and 50 dB, respectively.

Seen from Table 3, the fault location errors are kept within 0.833%. Because the fault current is relatively small when the monopole grounding fault occurs, the noise influence makes the fault location accuracy of the algorithm slightly reduced. With the increase of the fault transition resistance, the fault current further decreases, and the noise interference on the fault location accuracy is further intensified. Due to the randomness of white noise itself, there may be cases where some noises with lower SNR have larger fault location errors. However, with the decrease of noise intensity, the fault location errors generally present a downward trend.

In general, the new fault location algorithm proposed in this paper can still ensure high fault location accuracy in the case of noise interference.

TABLE 4. Fault location error under different sampling frequencies.

Sampling frequency /kHz	Fault distance /km	Transition resistance /Ω	Location results /km	K_{error} /%
10	1	0.1	0.9204	0.796
		1	0.9027	0.973
		10	0.8982	1.018
	5	0.1	4.9163	0.837
		1	4.8854	1.146
		10	4.8671	1.329
	9	0.1	8.9184	0.816
		1	8.8769	1.231
		10	8.8524	1.476
100	1	0.1	0.9606	0.394
		1	0.9344	0.656
		10	0.9292	0.708
	5	0.1	4.9575	0.425
		1	4.9261	0.739
		10	4.9248	0.752
	9	0.1	8.9583	0.417
		1	8.9263	0.737
		10	8.9256	0.744
200	1	0.1	0.9832	0.168
		1	0.9686	0.314
		10	0.9462	0.538
	5	0.1	4.9727	0.273
		1	4.9634	0.366
		10	4.9481	0.519
	9	0.1	8.9753	0.247
		1	8.9669	0.331
		10	8.9444	0.556

D. THE INFLUENCE OF SAMPLING FREQUENCY ON THE ACCURACY OF THE NEW ALGORITHM

The fault location methods based on the traveling wave have relatively high fault location accuracy, but these methods require high sampling frequency: the traveling wave fault location methods have a larger error at a lower sampling frequency. Table 4 shows the fault location results when the sampling frequency are 10kHz, 100kHz, and 200kHz, respectively. It can be seen from Table 4 that when the sampling frequency is reduced, the fault location accuracy of the algorithm decreases. At the sampling frequency of 10kHz, most of the fault location errors have exceeded the criterion K_{error}, indicating that this sampling frequency cannot accurately locate the fault.

In order to solve this problem, the idea of interpolation is introduced. Interpolation is an important method of discrete function approximation. It can be used to estimate the approximate value of the function at other points through the value of the function at a finite number of points. In the case of low sampling frequency, the interpolation of the original sampling points or fault location function can improve the fault location accuracy.

Therefore, in order to improve the fault location accuracy at a lower sampling frequency, this paper adopts cubic spline interpolation on the sampled data at 10kHz, and reduces the sampling interval to improve the fault location accuracy of the algorithm. Table 5 shows the fault location results

TABLE 5. Comparison of fault location error after cubic spline interpolation.

Interpolation condition	Fault distance /km	Transition resistance /Ω	Location results /km	K_{error}/%
Before	1	0.1	0.9204	0.796
		1	0.9027	0.973
		10	0.8982	1.018
	5	0.1	4.9163	0.837
		1	4.8854	1.146
		10	4.8671	1.329
	9	0.1	8.9184	0.816
		1	8.8769	1.231
		10	8.8524	1.476
After	1	0.1	0.9537	0.463
		1	0.9445	0.555
		10	0.9306	0.694
	5	0.1	4.9503	0.497
		1	4.9417	0.583
		10	4.9298	0.702
	9	0.1	8.9542	0.458
		1	8.9451	0.549
		10	8.9313	0.687

obtained by using cubic spline interpolation data. It can be seen from Table 5 that the errors of the fault location results after interpolation are reduced to a certain extent compared with that before interpolation, all fault location results at the sampling frequency of 10kHz are within the criterion K_{error}.

Therefore, the method proposed in this paper is not only suitable for high sampling frequency, but also can improve the fault location accuracy of the algorithm by cubic spline interpolation on the original data under the condition of low sampling frequency.

E. COMPARISON BETWEEN THE NEW ALGORITHM AND TRADITIONAL ALGORITHM

In order to verify the advantages of the proposed new algorithm, the traveling wave algorithm based on Pearson correlation coefficient (PCC) [23] is used to compare the fault location results. Table 6 shows the results of fault location error of PCC under the same fault. The results of Table 6 consist of various sampling frequency, fault distances, transition resistances, location results, and so on.

Table 7 shows the fault location errors of the algorithms based on PCC and the new algorithm when the fault occurs at 1km, and the shortened errors of the new algorithm compared to the method based on PCC. As can be seen in Table 7, the average shortened error is 27%. According to Table 6 and 7, the algorithm based on PCC has a higher degree of errors under the same conditions, which is extremely inappropriate in the short line distribution network. And it is very likely to cause the inability to determine the precise fault location.

The intuitive comparison of fault location errors between the algorithm based on PCC and the new algorithm based on Hausdorff distance in this paper under different sampling frequency is shown in Fig. 6. Fig. 6 shows the error

TABLE 6. Fault location error of algorithm based on PCC under the same fault.

Sampling frequency /kHz	Fault distance /km	Transition resistance /Ω	Location results /km	K_{error} /%
10	1	0.1	0.9265	0.735
		1	0.9154	0.846
		10	0.9028	0.972
	5	0.1	4.9259	0.741
		1	4.9139	0.861
		10	4.9042	0.958
	9	0.1	8.9271	0.729
		1	8.9145	0.855
		10	8.9036	0.964
100	1	0.1	0.9427	0.573
		1	0.9308	0.692
		10	0.9188	0.812
	5	0.1	4.9406	0.594
		1	4.9298	0.702
		10	4.9173	0.827
	9	0.1	8.9415	0.585
		1	8.9311	0.689
		10	8.9171	0.829
200	1	0.1	0.9698	0.302
		1	0.9512	0.488
		10	0.9365	0.635
	5	0.1	4.9683	0.317
		1	4.9521	0.479
		10	4.9371	0.629
	9	0.1	8.9679	0.321
		1	8.9518	0.482
		10	8.9362	0.638

TABLE 7. Comparison of fault location error between algorithm based on PCC and the new algorithm.

Sampling frequency /kHz	Transition resistance /Ω	K_{error} (PCC)/%	K_{error} (New algorithm)/%	Shortened error/%
10	0.1	0.735	0.463	37%
	1	0.846	0.555	34%
	10	0.972	0.694	28%
100	0.1	0.573	0.394	31%
	1	0.692	0.656	5%
	10	0.812	0.708	13%
200	0.1	0.302	0.168	44%
	1	0.488	0.314	36%
	10	0.635	0.538	15%

comparison of the two methods under different transition resistances. It can be clearly seen from Fig. 6 that the algorithm based on Hausdorff distance has significantly improved fault location accuracy compared with the algorithm based on PCC. This is due to the use of Hausdorff distance and cubic spline interpolation in this paper. The combination of Hausdorff distance and cubic spline interpolation is an effective data processing method, which reduces the fault location error of distribution lines, and has good fault location results under different transition resistances and different degrees of noise interference. Moreover, at lower sampling frequency, the matching degree of cubic spline interpolation and Hausdorff distance is higher, which greatly reduces the fault location error under low sampling frequency.

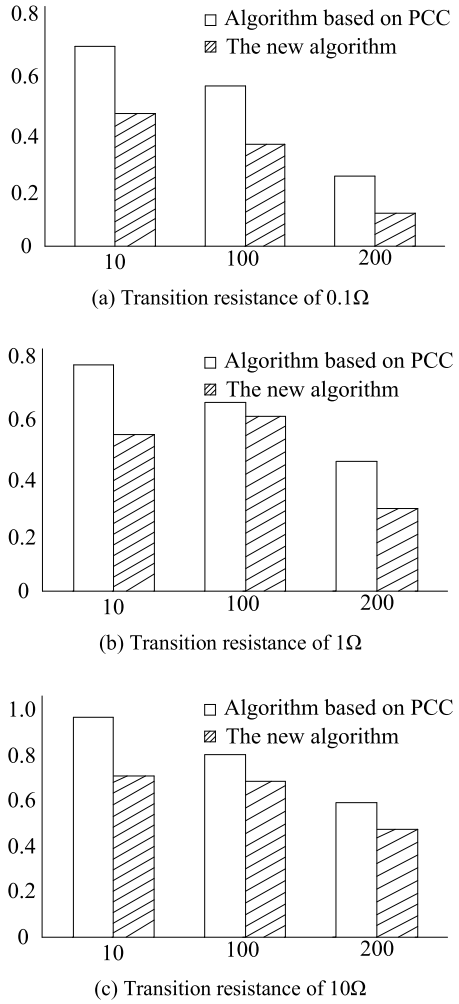

FIGURE 6. Comparison of fault location error between the traditional algorithm and the new algorithm.

V. CONCLUSION

This paper proposes a new fault location algorithm for VSC based DC distribution networks. Based on the similarity between the forward and reverse traveling wave differential current waveforms, the Hausdorff distance algorithm is used to characterize the similarity between the two waveforms, and extract the fault location information. By performing cubic spline interpolation on the waveform data, the fault location error of the algorithm is reduced to a certain extent, and the fault location accuracy is improved:

(1) The method proposed in this paper is less affected by transition resistance and sampling frequency, which has strong anti-noise interference ability, and can accurately locate faults on the entire line.

(2) The Hausdorff distance algorithm is used to analyze the correlation between the shifted forward difference current and reverse difference current, and the highest degree of correlation is the fault location. The location principle of the criterion is clear, and it is easy to judge whether the fault location is successful or not.

(3) The cubic spline interpolation method interpolates the data at low sampling frequency to fit a smooth waveform, which significantly reduces the fault location error and overcomes the limitation of sampling frequency on traveling wave fault location method.

REFERENCES

[1] R. Lobenstein and C. Sulzberger, "Eyewitness to DC history," *IEEE Power Energy Mag.*, vol. 6, no. 3, pp. 84–90, May/Jun. 2008.
[2] M. E. Baran and N. R. Mahajan, "DC distribution for industrial systems: Opportunities and challenges," *IEEE Trans. Ind. Appl.*, vol. 39, no. 6, pp. 1596–1601, Nov./Dec. 2003.
[3] R. Sharma, Q. Wu, S. T. Cha, K. H. Jensen, T. W. Rasmussen, and J. Østegaard, "Power hardware in the loop validation of fault ride through of VSC HVDC connected offshore wind power plants," *J. Mod. Power Syst. Clean Energy*, vol. 2, no. 1, pp. 23–29, Mar. 2014.
[4] H. Sun, L. Du, and G. Liang, "Calculation of electromagnetic radiation of VSC-HVdc converter system," *IEEE Trans. Magn.*, vol. 52, no. 3, pp. 1–4, Mar. 2016.
[5] V. L. Merlin, R. C. D. Santos, S. Le Blond, and D. V. Coury, "Efficient and robust ANN-based method for an improved protection of VSC-HVDC systems," *IET Renew. Power Gener.*, vol. 12, no. 13, pp. 1555–1562, Oct. 2018.
[6] B. Chang, O. Cwikowski, M. Barnes, R. Shuttleworth, A. Beddard, and P. Coventry, "Review of different fault detection methods and their impact on pre-emptive VSC-HVDC DC protection performance," *High Voltage*, vol. 2, no. 4, pp. 211–219, Dec. 2017.
[7] B. Li, M. Lv, B. Li, S. Xue, and W. Wen, "Research on an improved protection principle based on differential voltage traveling wave for VSC-HVDC transmission lines," *IEEE Trans. Power Del.*, vol. 35, no. 5, pp. 2319–2328, Oct. 2020.
[8] K. De Kerf, K. Srivastava, M. Reza, D. Bekaert, S. Cole, D. Van Hertem, and R. Belmans, "Wavelet-based protection strategy for DC faults in multi-terminal VSC HVDC systems," *IET Gener. Transmiss. Distrib.*, vol. 5, no. 5, pp. 496–503, May 2011.
[9] J. Sneath and A. D. Rajapakse, "Fault detection and interruption in an earthed HVDC grid using ROCOV and hybrid DC breakers," *IEEE Trans. Power Del.*, vol. 31, no. 3, pp. 973–981, Jun. 2016.
[10] M. E. Baran and N. R. Mahajan, "Overcurrent protection on voltage-source-converter-based multiterminal DC distribution systems," *IEEE Trans. Power Del.*, vol. 22, no. 1, pp. 406–412, Jan. 2007.
[11] J. Liu, N. Tai, and C. Fan, "Transient-voltage-based protection scheme for DC line faults in the multiterminal VSC-HVDC system," *IEEE Trans. Power Del.*, vol. 32, no. 3, pp. 1483–1494, Jun. 2017.
[12] C. Zhang, G. Song, L. Yang, and X. Dong, "Non-unit travelling wave protection method for DC transmission line using waveform correlation calculation," *IET Gener., Transmiss. Distrib.*, vol. 14, no. 12, pp. 2263–2270, Jun. 2020.
[13] Y. Zhang, N. Tai, and B. Xu, "Fault analysis and traveling-wave protection scheme for bipolar HVDC lines," *IEEE Trans. Power Del.*, vol. 27, no. 3, pp. 1583–1591, Jul. 2012.
[14] D. Wang, D. Yu, H. Yang, M. Hou, and Y. Guo, "Novel travelling wave directional pilot protection for VSC-HVDC transmission line," *IET Gener., Transmiss. Distrib.*, vol. 14, no. 9, pp. 1705–1713, May 2020.
[15] C. Zheng, D. Xinzhou, and L. Chengmu, "Robustness of one-terminal fault location algorithm based on power frequency quantities," in *Proc. IEEE Power Eng. Soc. Summer Meeting*, vol. 3, Chicago, IL, USA, Jul. 2002, pp. 1118–1122.
[16] W. Wang, M. Barnes, O. Marjanovic, and O. Cwikowski, "Impact of DC breaker systems on multiterminal VSC-HVDC stability," *IEEE Trans. Power Del.*, vol. 31, no. 2, pp. 769–779, Apr. 2016.
[17] Z.-Y. He, K. Liao, X.-P. Li, S. Lin, J.-W. Yang, and R.-K. Mai, "Natural frequency-based line fault location in HVDC lines," *IEEE Trans. Power Del.*, vol. 29, no. 2, pp. 851–859, Apr. 2014.
[18] A. Swetapadma and A. Yadav, "Improved fault location algorithm for multi-location faults, transforming faults and shunt faults in thyristor controlled series capacitor compensated transmission line," *IET Gener., Transmiss. Distrib.*, vol. 9, no. 13, pp. 1597–1607, Oct. 2015.
[19] M. Farshad and J. Sadeh, "A novel fault-location method for HVDC transmission lines based on similarity measure of voltage signals," *IEEE Trans. Power Del.*, vol. 28, no. 4, pp. 2483–2490, Oct. 2013.

[20] A. Sadegh, A. Saeed, and S. P. Majid, "Fault location on multi-terminal DC systems using synchronized current measurements," *Int. J. Electr. Power Energy Syst.*, vol. 63, pp. 779–786, Dec. 2014.
[21] S. Shi, A. Lei, X. He, S. Mirsaeidi, and X. Dong, "Travelling waves-based fault location scheme for feeders in power distribution network," *J. Eng.*, vol. 2018, no. 15, pp. 1326–1329, Oct. 2018.
[22] L. BIN, Z. Jihang, L. Haijin, and R. Ye, "Fault location of HVDC transmission lines based on waveform similarity analysis," *Electr. Power Automat. Equip.*, vol. 39, no. 9, pp. 27–32 and 53, 2019.
[23] X. Zhang, N. Tai, P. Wu, C. Fan, X. Zheng, and W. Huang, "A new theory for locating line fault in power system: Simulation part," *IEEE Access*, vol. 7, pp. 93858–93870, 2019.
[24] A. A. Taha and A. Hanbury, "An efficient algorithm for calculating the exact Hausdorff distance," *IEEE Trans. Pattern Anal. Mach. Intell.*, vol. 37, no. 11, pp. 2153–2163, Nov. 2015.
[25] O. Schutze, X. Esquivel, A. Lara, and C. A. C. Coello, "Using the averaged Hausdorff distance as a performance measure in evolutionary multiobjective optimization," *IEEE Trans. Evol. Comput.*, vol. 16, no. 4, pp. 504–522, Aug. 2012.
[26] F. V. Lopes, "Settings-free traveling-wave-based Earth fault location using unsynchronized two-terminal data," *IEEE Trans. Power Del.*, vol. 31, no. 5, pp. 2296–2298, Oct. 2016.
[27] A. M. Bica, "Fitting data using optimal Hermite type cubic interpolating splines," *Appl. Math. Lett.*, vol. 25, no. 12, pp. 2047–2051, 2012.
[28] Y. Bai and D. Wang, "On the comparison of trilinear, cubic spline, and fuzzy interpolation methods in the high-accuracy measurements," *IEEE Trans. Fuzzy Syst.*, vol. 18, no. 5, pp. 1016–1022, Oct. 2010.
[29] X. Wang, G. Song, J. Gao, X. Wei, Y. Wei, K. Mostafa, Z. Hu, and Z. Zhang, "High impedance fault detection method based on improved complete ensemble empirical mode decomposition for DC distribution network," *Int. J. Electr. Power Energy Syst.*, vol. 107, pp. 538–556, May 2019.
[30] Y.-Y. Zhang and J.-K. Zhang, "Fundamental applicability of spatial modulation: High-SNR limitation and low-SNR advantage," *IEEE J. Sel. Areas Commun.*, vol. 37, no. 9, pp. 2165–2178, Sep. 2019.

YANFANG WEI received the B.Sc. and M.Sc. degrees in electrical engineering from Henan Polytechnic University, Jiaozuo, China, in 2006 and 2008, respectively, and the Ph.D. degree in electrical engineering from Hohai Univsersity, Nanjing, China, in 2012. He is currently an Associate Professor with Henan Polytechnic University. His current research interests include flexible dc transmission and power system analysis.

PENGYU SUN received the B.Sc. degree in electrical engineering from the Zhengzhou University of Aeronautics, Zhengzhou, China, in 2018. He is currently pursuing the M.Sc. degree in electrical engineering with Henan Polytechnic University, Jiaozuo, China. His main research interests include protection and control of power system and fault location technology of VSC-HVDC.

ZHUOLIANG SONG received the B.Sc. degree in electrical engineering from Henan Polytechnic University, Jiaozuo, China, and North Carolina Agricultural and Technical State University, Greensboro, NC, USA, in 2020. He is currently pursuing the M.Sc. degree in electrical engineering with the University of Southern California, Los Angeles, CA, USA. His current research interests include power signal processing, fault detection and demand response in power systems.

PENG WANG (Member, IEEE) received the Ph.D. degree in electrical engineering from Shanghai Jiao Tong University, Shanghai, China, in 2014. He is currently a Senior Engineer with the Electric Power Research Institute, State Grid Henan Electric Power Company, Zhengzhou, China. His research interests is the application of new technology and new equipment in distribution networks.

ZHIHUI ZENG received the B.Sc. and M.Sc. degrees in electrical engineering from Henan Polytechnic University, Jiaozuo, China, in 2002 and 2008, respectively, and the Ph.D. degree in measurement technology and automatic equipment from the Beijing University of Technology, Beijing, China, in 2016. He is currently an Associate Professor with Henan Polytechnic University. His current research interests include electronics technology in clean energy power field.

XIAOWEI WANG (Member, IEEE) received the B.Sc. and M.Sc. degrees in electrical engineering from Henan Polytechnic University, Jiaozuo, China, in 2006 and 2011, respectively. He is currently pursuing the Ph.D. degree with the School of Electrical Engineering, Xi'an Jiaotong University, Xi'an, China. He is also a Lecturer with Henan Polytechnic University. His main research interests include fault location, power system protection, and power signal processing.